Heliyon 10 (2024) e40111

Contents lists available at ScienceDirect

Heliyon

journal homepage: www.cell.com/heliyon

Research article

Numerical study of effective parameters on deformation and coalescence of ferrofluid droplets under uniform magnetic field

Mobina Taghaddosi, Mobin Salehi, Borhan Beigzadeh *

Biomechatronics and Cognitive Engineering Research Lab, School of Mechanical Engineering, Iran University of Science and Technology, Tehran, Iran

A R T I C L E I N F O

Keywords:
Ferrofluid
Multiphase flow
Magnetic field
Conservative level set method
Coalescence

A B S T R A C T

This research examines different numerical techniques for modeling ferrofluids in a non-magnetic liquid subjected to homogeneous and steady magnetic field. It particularly compares the conservative level set method with the Volume of Fluid (VOF) and Simple Coupled Level Set and Volume of Fluid (SCLSVOF) methods. By comparing these methods with experimental data, we established the superiority of the utilized method in this study. Several case studies were conducted to evaluate how a homogeneous magnetic actuation affects ferrofluid dynamics, considering parameters such as initial droplet size, surface tension coefficient, and magnetic susceptibility. Additionally, the study explored the coalescence of two falling ferrofluid droplets under the combined effects of an external magnetic field and gravity. The conservative level set method was shown to be extendable to three-dimensional environments, unlike the standard level set method. The novelty of this work lies in demonstrating that the conservative level set method is particularly effective for ferrofluids, accurately capturing their complex dynamics. The main novelty of this article lies in demonstrating the precision of Conservative Level Set Method while utilizing a reduced number of equations compared to other works. This reduction in complexity enhances the method's efficiency without compromising precision, making it especially suited for applications requiring both speed and accuracy, such as model-based control systems.

1. Introduction

Ferrofluid is a stable liquid mixture made up of nano scaled paramagnetic particles dispersed in another liquid. Each particle is coated with a thin layer to stop them from sticking together. Developed in the early 1960s, ferrofluids were initially used as additives in rocket fuel. Their popularity grew as the unique properties of magnetic fluids for remote control via magnetic actuation were better understood [1]. Today, ferrofluids are applied in various engineering and biomedical fields [2], including enhancing heat transfer and mass transfer performance [3–6], serving as viscous dampers in bearings and magnetic sealants [7], functioning as tools in lab-on-chip devices [8,9], and enabling targeted drug delivery [10]. Using ferrofluids, microrobots can enhance drug delivery to specific areas, thereby minimizing the potential side effects in other parts of the body [11]. By manipulating the shape and position of ferrofluid robots using a magnetic actuation, it is possible to develop microrobots that can be controlled wirelessly. These microrobots can be used to target cancerous tumors that are hard to reach [12]. They are also useful for performing minimally invasive surgeries, which help reduce the risk of infection and shorten recovery times [13]. Additionally, they can aid in targeted drug delivery [14]. Other research has also explored the use of magnetic particles for delivering drugs to specific targets [15–17]. To magnetically control the

* Corresponding author.
E-mail address: b_beigzadeh@iust.ac.ir (B. Beigzadeh).

https://doi.org/10.1016/j.heliyon.2024.e40111
Received 15 July 2024; Received in revised form 22 October 2024; Accepted 1 November 2024
Available online 4 November 2024
2405-8440/© 2024 The Authors. Published by Elsevier Ltd. This is an open access article under the CC BY-NC license (http://creativecommons.org/licenses/by-nc/4.0/).

form and location of a ferrofluidic robot, it is crucial first to develop model's dynamic of the ferrofluid droplet and simulate its behavior. This simulation enables the implementation of the controller in the subsequent step [18]. Shyam et al. [19] conducted both experimental and numerical investigations on the impact of a variable magnetic field on ferrofluid droplets. They reported that the magnetic field induces flow instability, and the magnetic particles exhibit complex spatio-temporal dynamics, which could be applied to rapid droplet mixing. The droplet's behavior and dynamics can be studied by exposing it to a magnetic field. Numerous experimental tests and numerical simulations have been conducted to understand how ferrofluid behaves When placed in a non-magnetic liquid under this type of field. Given the considerable challenge of tracking the moving interface of the ferrofluid droplet with the encompassing fluid, numerical methods are required. The following section reviews the numerical methods proposed in recent decades.

In a study by Flament et al. [20] in 1996, the deformation of a ferrofluid droplet in water was experimentally observed under a homogeneous magnetic field with different intensities. Lee et al. [21] were the first to investigate the deformation of two gas bubbles with identical radii in ferrofluid exposed to a homogeneous magnetic field. Lavrova et al. [22] Used the finite element method and analyzed the configuration of a ferrofluid droplet held in place by surface tension forces and a magnetic field. In recent decades, numerous numerical techniques created for monitoring and establishing the position of the interface. Throughout, the level set method, introduced by Osher and Sethian [23], is widely recognized. Liu et al. [24] studied the impact of a homogeneous magnetic field on the generation of ferrofluid droplets in a flow-focusing channel for interface tracking using both the finite volume method and the level set method. Cunha et al. [25] utilized the level set method to model the variation of a two-dimensional ferrofluid droplet subjected to both a homogeneous magnetic field and shear flow, and also investigated the breakup of ferrofluid droplets undergoing significant deformations. Shyam et al. [26] conducted research on the disintegration behavior of ferrofluid droplets and verified the controllability of breakup process by varying the magnetic field within a T-shaped lab-on-a-chip device. Hassan et al. [27] Studied the distortion of a ferrofluid when subjected to a shear flow while exposed to a homogeneous magnetic actuation. They verified that employing the level set method can model the droplet's dynamic interface motion. Additionally, Abicalil et al. [28] used the level set method to simulate the behavior of a solitary ferrofluid bead in three dimensions when subjected to simple shear flows and homogeneous magnetic fields.

Ferrofluids subjected to a homogeneous magnetic field have been studied using other numerical techniques, including the volume of fluid (VOF) and lattice Boltzmann methods. Afkhami et al. [29] used the VOF method to numerically model the motion and deformation of a ferrofluid exposed to external magnets within a weakly magnetic liquid. Hu et al. [30] employed the lattice Boltzmann method to simulate the shape-shifting of a ferrofluid bead and the merging of bubbles within the ferrofluid. Zhang et al. [31] examine the deformation behavior of ferrofluid droplets positioned between air and a liquid when subjected to a vertical homogeneous magnetic field. This study utilizes an advanced generalized conservative phase-field lattice Boltzmann approach. He et al. [32] developed a hybrid method combining the immersed interface technique with the phase-field Boltzmann model to simulate the behavior of ferrofluids, employing a phase-field-based approach to model the magnetic potential. Their method effectively captures key phenomena, such as droplet deformation and bubble merging under magnetic and shear forces, while demonstrating high numerical stability and applicability.

Several researchers have developed new simulations of the effects of magnetic fields on ferrofluids by combining numerical methods. Shi et al. [33] introduced the VOSET method, which integrates the Volume of Fluid (VOF) approach with the Level Set technique. They investigate how magnetic fields and dimensionless numbers—such as the Bond, Weber, and Reynolds numbers—affect ferrofluid droplet dynamics. They further modeled the behavior of a ferrofluid droplet descending through a weakly magnetic fluid while subjected to a homogeneous magnetic field. VOSET method, initially presented by Sun and Tao [34], was employed to simulate incompressible two-phase flow in the absence of heat transfer. Albadawi et al. [35] improved surface tension models by integrating the Level Set method with the Volume of Fluid (VOF) approach, resulting in the development of the S-CLSVOF and Simple Couple Level Set methods. Ghaffari et al. [36] employed this approach to simulate and validate shape-shifting of ferrofluid droplet exposed to external magents, comparing their results with the experimental findings of Afkhami et al. [37]. Chen et al. [38] developed a simplified multiphase lattice Boltzmann method (SMLBM) to address the limitations of standard lattice Boltzmann methods and to simulate incompressible multiphase flows having significant density ratios. They applied this approach to scenarios such as air bubbles rising in water and problems involving large interface deformations. Khan et al. [39] analyzed the impact of the separation distance between the centers of two ferrofluid droplets on their coalescence and the impact of homogeneous magnetic field on droplet deformation using SMLBM and a self-correcting method. Majidi et al. [40] utilized a hybrid lattice Boltzmann-finite difference method to investigate the deformation of a ferrofluid droplet within another droplet subjected to homogeneous magnetic fields and shear flow. This method integrates a conservative phase-field lattice Boltzmann approach with finite difference calculations for the magnetic field.

In the current study, we use COMSOL software to investigate how various parameters affect the shape of a ferrofluid. The dynamics and behavior of the system under different conditions are analyzed using the conservative level set method provided by the software, enabling us to wirelessly control the droplet's shape via magnetic fields.

The structure of the paper is as follows: Section 2 discusses the materials and numerical methods, while Section 3 details the governing equations of fluids and magnetism. Section 4 validates our simulation results in comparison to empirical findings to ensure precision. Upon confirming the results, we examine the impact of different parameters on the shape transformation of the ferrofluid droplet in 2D mode, comparing these findings with the S-CLSVOF numerical method. We also explore the merging of two ferrofluid droplets under homogeneous magnetic fields and gravity, and present a 3D model of the droplet subjected to different magnetic field intensities. Finally, Section 6 outlines potential future research directions.

2. Material and methods

This study involves the development of a numerical model aimed at examining the behavior and dynamics of a ferrofluid droplet subjected to a homogeneous magnetic field. The 2D system consists of a ferrofluid droplet immersed in a non-magnetic, incompressible, laminar flow, creating a two-phase flow environment. When subjected to a homogeneous magnetic field, the ferrofluid droplet becomes magnetized, which changes the surrounding uniform magnetic field into a non-uniform one [41]. As a result, a magnetic field gradient arises around the droplet. Since magnetic force originates from this gradient, it causes the droplet to deform and tracking the deformation and boundary movement of the droplet requires a numerical approach. The level set method, as proposed in previous studies [42], is employed here to capture the interface dynamics of the two-phase flow, and this approach is explored in the following sub-section.

2.1. Conservative level set method for interface tracking

One of downsides of traditional level set methods is their non-conservative nature, which can lead to undesirable mass loss or gain in incompressible two-phase flows, resulting in physically inaccurate response [43]. To address this issue, Olsson and Kreiss introduced a conservative level set method designed to track moving interfaces in a velocity field without the inevitable divergence that typically occurs in two-phase flows [44].

In our simulation, the conservative level set method was employed to monitor the interface between the ferrofluid droplet and the weakly magnetic fluid. This method employs an auxiliary scalar function, ϕ, known as the level set function. This value smoothly transitions between 0 and 1 across the interface, where it equals 0 in one domain, 1 in the other, and takes a value of 0.5 at the interface.

The method is governed by Eq. (1):

$$\frac{\partial \phi}{\partial t} + \boldsymbol{u}.\nabla\phi = \gamma\nabla.\left(\varepsilon\nabla\phi - \phi(1-\phi)\frac{\nabla\phi}{|\nabla\phi|}\right) \tag{1}$$

where $\boldsymbol{u}$ is the velocity field, γ and ε are stabilization parameters; γ is the reinitialization parameter and and corresponds to the peak velocity within the flow, and ε is the controlling interface thickness parameter in meter.

The two-phase flow properties for the laminar flow and magnetic field must first be derived using the level set function. Using the level set function, we apply linear interpolation, as defined in Eqs. (2)–(5), to incorporate the density (ρ), dynamic viscosity (η), magnetic permeability (μ), and magnetic susceptibility (χ) of the fluid.

$$\rho = \rho_c + (\rho_d - \rho_c)\,\phi \tag{2}$$

$$\eta = \eta_c + (\eta_d - \eta_c)\,\phi \tag{3}$$

$$\mu = \mu_c + (\mu_d - \mu_c)\,\phi \tag{4}$$

$$\chi = \chi_c + (\chi_d - \chi_c)\,\phi \tag{5}$$

The subscripts c represents continuous phase and d express the droplet phase.

3. Governing equations

Our system consists of an incompressible, isothermal ferrofluid suspended in another isothermal, incompressible, immiscible medium subjected to homogeneous magnetic field. To derive the governing equations, we apply the continuity equation along with the Navier-Stokes momentum equations according to Eqs. (6) and (7):

$$\nabla.\boldsymbol{u} = 0 \tag{6}$$

$$\frac{\partial(\rho\boldsymbol{u})}{\partial t} + \nabla.(\rho\boldsymbol{u}\boldsymbol{u}) = -\nabla p + \nabla.[\tau] + \boldsymbol{F}_\sigma + \boldsymbol{F}_m \tag{7}$$

where ρ shows density and is derived from Eq.2, p stands for the pressure and τ represents the viscous stress tensor.

The viscous stress tensor ($[\tau]$) is described as Eq. (8):

$$[\tau] = \left[\eta\left(\nabla\boldsymbol{u} + (\nabla\boldsymbol{u})^T\right)\right] \tag{8}$$

where η shows dynamic viscosity and is derived from Eq. (3). The volume forces on the right-hand side of Eq. (7) are surface tension ($\boldsymbol{F}_\sigma$) and magnetic force ($\boldsymbol{F}_m$), respectively.

The force due to surface tension ($\boldsymbol{F}_\sigma$)) is described by Eq. (9):

$$\boldsymbol{F}_\sigma = \nabla.\left[\sigma\left\{\mathbf{I} + \left(-\boldsymbol{n}\boldsymbol{n}^T\right)\right\}\delta\right] \tag{9}$$

where σ represents the surface tension coefficient, $\mathbf{I}$ denotes the identity matrix, δ refers to the Dirac delta function, and vector $\boldsymbol{n}$ denotes the normalized perpendicular direction to the interface., which is expressed using the level set function as $\boldsymbol{n} = \frac{\nabla\phi}{|\nabla\phi|}$.

The magnetic force is incorporated into the Navier-Stokes equation to couple the laminar flow and magnetic field modules (see Supplementary Information). This force can be related to the magnetic stress tensors through Eq. (10):

$$\boldsymbol{F}_m = \nabla.[\tau_m] \tag{10}$$

The magnetic stress tensor (τ_m) for the mentioned medium under an applied magnetic field is given by $\tau_m = -\frac{\mu}{2}H^2[\boldsymbol{I}] + \mu\ \mathbf{HH}^T$ [1] where H is the magnitude of the magnetic field intensity $\mathbf{H}$. By expanding the magnetic tension tensor and utilizing Eq. (4), the resulting magnetic force can be represented as Eq. (11):

$$\boldsymbol{F}_m = \nabla.\tau_m = \nabla.\ \mu \begin{bmatrix} \mathbf{H}_x^2 - \frac{1}{2}H^2 & \mathbf{H_xH_y} \\ \mathbf{H_xH_y} & \mathbf{H}_\mathbf{y}^2 - \frac{1}{2}H^2 \end{bmatrix}$$

$$= (\mu_c + (\mu_d - \mu_c)\,\phi) \begin{bmatrix} \dfrac{\partial(H_x^2 - \frac{1}{2}H^2)}{\partial x} + \dfrac{\partial(H_xH_y)}{\partial y} \\ \dfrac{\partial(H_yH_x)}{\partial x} + \partial(H_y^2 - \frac{1}{2}H^2)\Big/\partial y \end{bmatrix} \tag{11}$$

Considering the linearity and homogeneity of the material, the magneto-static Maxwell equations establish connections between magnetic field intensity $\mathbf{H}$, magnetization $\mathbf{M}$, and magnetic flux density $\mathbf{B}$ through Eqs. (12) and (13):

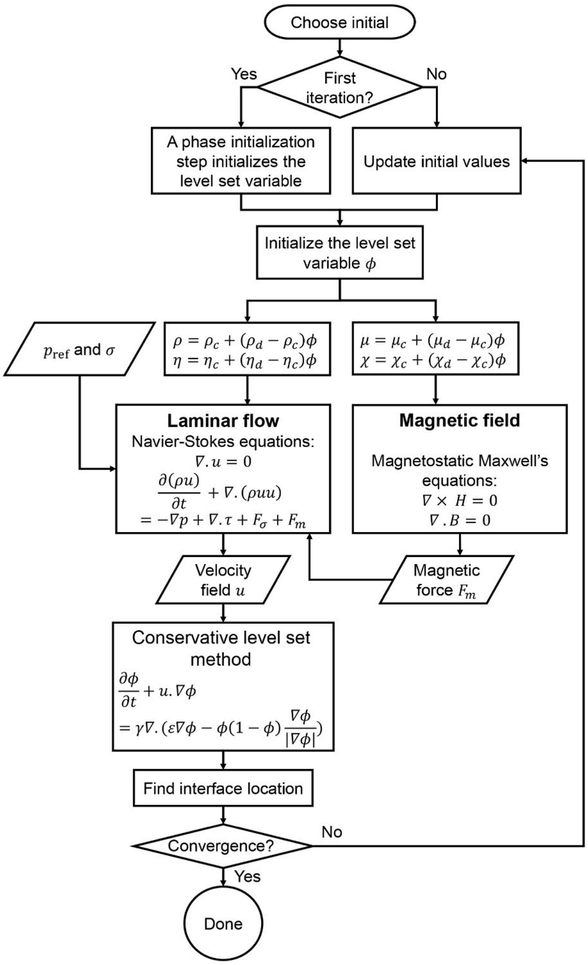

Fig. 1. Simulation flowchart of ferrofluid droplet deformation.

$$\nabla \times \mathbf{H} = 0, \mathbf{M} = \chi \mathbf{H} \tag{12}$$

$$\nabla . \mathbf{B} = 0 \tag{13}$$

B is calculated through Eq. (14):

$$\mathbf{B} = \begin{cases} \mu_0(\mathbf{H} + \mathbf{M}) = \mu_0(1+\chi)\mathbf{H} \\ \mu_0\mathbf{H} \end{cases} \tag{14}$$

in the ferrofluid domain in the non-magnetic medium fluid domain.

here, $\mu_0 = 4\pi \times 10^{-7} H/m$ is the magnetic permeability of vacuum, and χ is the magnetic susceptibility and is derived from Eq. (5), which is described by Eq. (15):

$$\chi = \mu_r - 1 \tag{15}$$

where μ_r is relative magnetic permeability. Moreover, for comparative analysis, we utilize a dimensionless quantity known as the magnetic Bond number. This number characterizes the relationship between the magnetic force and the surface tension force, and can be expressed as Eq. (16) [45]:

$$Bo_m = \frac{\mu_0 H_0^2}{\sigma \kappa_0} \tag{16}$$

where H_0 is magnetic field intensity due to external magnets and κ_0 is the curvature of the initial shape of the ferrofluid droplet of initial radius R_0, respectively, where $\kappa_0 = \frac{2}{R_0}$. The simulation flowchart for shape transformation of the ferrofluid droplet, as described in this section, is shown in Fig. 1.

4. Validation

To validate our simulation results obtained using COMSOL with the empirical findings published by Afkhami et al. [37], we conducted our simulation under the same conditions as those of the experimental study. Therefore, our model consists of an immiscible, isothermal, and incompressible ferrofluid droplet surrounded by a non-magnetic fluid subjected to homogeneous magnetic field.

In this case study, the ferrofluid droplet with a constant magnetic susceptibility $\chi = 0.8903$ and an initial radius of $R_0 = 1.291$ mm is located in the center of a square of length $15R_0$ (Fig. 2A). The surface tension coefficient is set to be 0.0135 N/m. The fluids are characterized by a density of 1260 kg/m3 and a viscosity of 0 .1 Pa s for both.

To ensure a reliable computational grid, a mesh independency study is conducted. We use a triangular mesh type for the fluid domain and a quadrilateral mesh type for the boundaries to construct the computational grid (see Supplementary Fig. S1). The shape transformation of the droplet subjected to a homogeneous magnetic actuation with an intensity of $H_0 = 5960 \frac{A}{m}$ is calculated for five different mesh grids; the direction and magnitude of this magnetic field are shown in Fig. 2B. Subsequently, the droplet aspect ratio from each simulation is evaluated against the experimental findings using Eq. (17):

$$Relative\ error\ (\%) = \left| \frac{\left(\frac{b}{a}\right)_{exp} - \left(\frac{b}{a}\right)_{sim}}{\left(\frac{b}{a}\right)_{exp}} \right| \times 100 \tag{17}$$

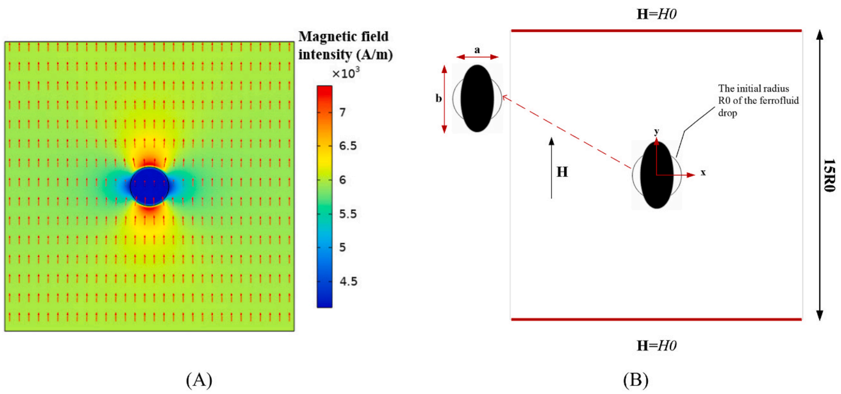

Fig. 2. Simulation model of a ferrofluid droplet subjected to a homogeneous magnetic field. (A) Magnetic field. (B) Geometry model.

The relative error in Eq. (17) is calculated by experimental values of the droplet shape (aspect) ratio $\left(\frac{b}{a}\right)_{exp}$ and the simulation values of the droplet aspect ratio $\left(\frac{b}{a}\right)_{sim}$. As illustrated in Fig. 3, increasing the total number of mesh elements beyond 60,298 results in no change in the relative error, which remains constant at 1.15 %.

Furthermore, the model was tested under external uniform magnetic fields with varying intensities. In addition to validating the results against those obtained by Afkhami et al. [37], our model was also compared with the VOF and S-CLSVOF methods reported by Ghaffari et al. [36]. The simulation results, shown in Fig. 4, indicate that the maximum deviation between our results and the experimental data is 2.06 %. In contrast, the deviations for the VOF and S-CLSVOF methods are 14.97 % and 10.24 %, respectively. This demonstrates a strong agreement between our results and the experimental data, even at higher magnetic field intensities. Thus, the conservative level set method proves to be effective for interface tracking in the simulation of a ferrofluid droplet surrounded by a weakly magnetic fluid.

5. Results and discussion

In this part of the study, the influence of various parameters on the deformation of a ferrofluid droplet subjected to a homogeneous magnetic field is examined. As outlined in Section 3, changes in the droplet's behavior can be expressed by the dimensionless Bond number, which depends on factors such as magnetic field intensity, the droplet's initial radius, and the surface tension coefficient—all of which influence the deformation. Additionally, at a constant Bond number, the magnetic susceptibility of ferrofluid, plays an essential role in determining droplet shape-shifting exposed to external magnets. The effects of these parameters are simulated and presented below, along with a comparison to the S-CLSVOF numerical method used by Ghaffari et al. [36].

Before examining the behavior of the ferrofluid under the specified parameters, we must first determine time influence on the equilibrium form of ferrofluid when subjected to a homogeneous magnetic field. Initially, the droplet is influenced solely by surface tension forces. However, once exposed to the homogeneous magnetic field, the forces induced by the magnetic field exceed those exerted by surface tension. Consequently, the droplet extends along the axis of the magnetic field and continues to change shape until the surface tension equals to magnetic forces (see Supplementary Fig. S4). The deformation of the droplet under a magnetic field intensity of $H_0 = 5960$ A/m over a period of 1 s is shown in Fig. 5.

As illustrated in Fig. 6, the surface tension and magnetic forces reach equilibrium state at 0.1 s in the COMSOL simulation. In the simulation, the time step is set to 0.01 s.

5.1. Magnetic field intensities impact on the deformation of ferrofluid

This segment examines the influence of magnetic field intensity on the form of the ferrofluid droplet. All other factors, such as the initial droplet radius, surface tension, and magnetic susceptibility, remain constant as described in Section 4. As a result, based on Eq. (16), the Bond number increases as the magnetic field intensity rises. Fig. 7 indicates that higher magnetic field intensities result in increased deformation of the droplet.

For a more detailed examination of the correlation of the shape ratio and the Bond number, we will refer to the theory presented by Afkhami et al. [37]. The shape ratio in relation to the magnetic Bond number, held constant at specific magnetic susceptibility values (χ), is expressed by Eq. (18) [37]:

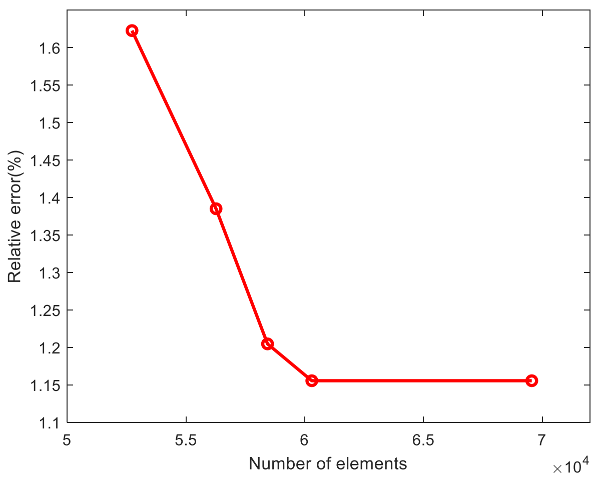

Fig. 3. Mesh independency study results.

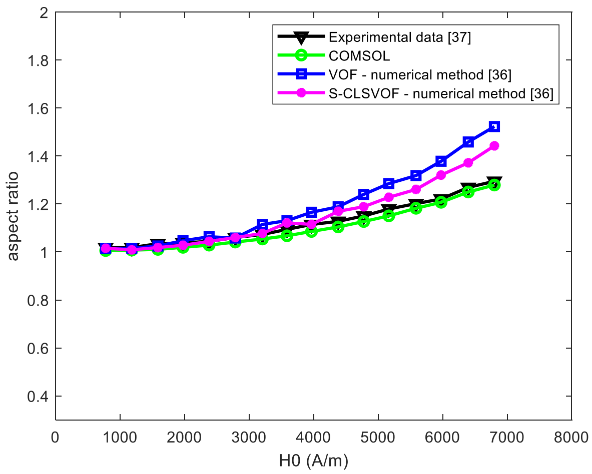

Fig. 4. A comparison between COMSOL simulation with two numerical methods and experimental data subjected to various magnetic field intensities.

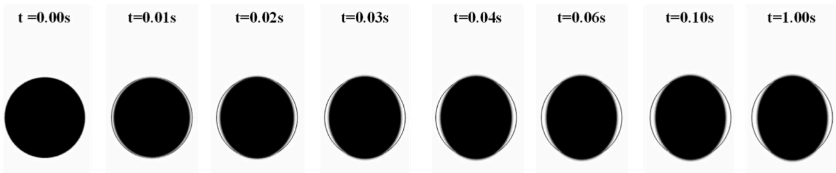

Fig. 5. The ferrofluid deformation subjected to homogeneous magnetic field in 1 s.

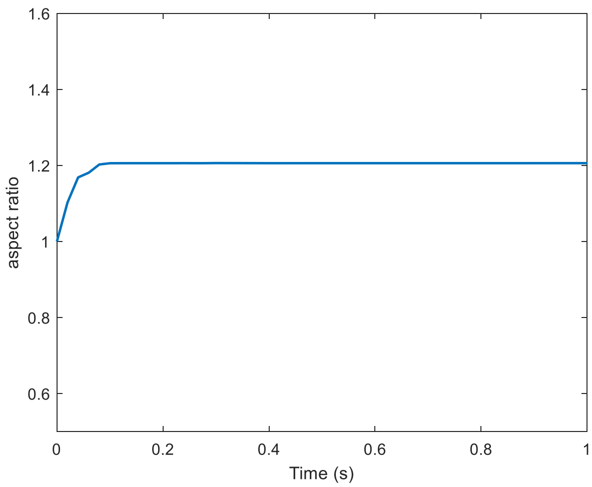

Fig. 6. The diagram of the stabilization phase of the ferrofluid droplet's deformation when subjected to a homogeneous magnetic field.

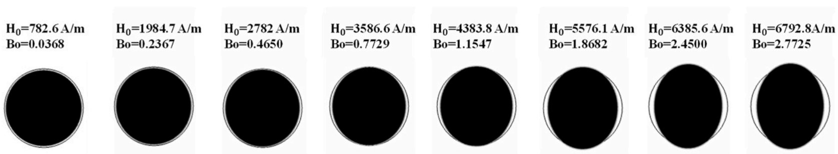

Fig. 7. Schematic of the ferrofluid shape transformation subjected to different homogeneous magnetic field intensities.

$$Bo_m = \left[\frac{1}{\chi} + k\right]^2 \left(\frac{b}{a}\right)^{\frac{1}{3}} \left(2\frac{b}{a} - \left(\frac{b}{a}\right)^{-2} - 1\right) \tag{18}$$

where k is the demagnetizing factor.

The shape ratio of the deformed ferrofluid droplet, simulated for various Bond numbers with constant magnetic susceptibility, is compared with theoretical values obtained from Eq. (18) and shown in Fig. 8. As demonstrated, the simulation findings are in strong agreement with the theoretical predictions outlined in Equation (18). However, as the Bond number increases, the discrepancy between the simulation and the theoretical values grows. This discrepancy is due to the deviations of Eq. (18) from the experimental results reported by Afkhami et al. [37]. Our simulation findings, which closely correspond with the experimental data (see Fig. 4), suggest that Eq. (18) exhibits similar deviations from our simulations as well.

5.2. The impact of different initial radii on the shape-shifting of ferrofluid

The initial radius of the ferrofluid droplet significantly impacts its deformation. According to Eq. (16), the effect of this parameter correlates positively with the droplet's shape ratio, which is the ratio of the larger to the smaller radius of the deformed ellipse. As the initial radius increases, the magnetic forces become more prominent compared to the surface tension forces, leading to greater deformation and a higher aspect ratio (see Supplementary Fig. S5). Conversely, when the initial radius is less than 0.5 mm, surface tension forces dominate, and droplet deformation is minimal. Fig. 9 illustrates the simulation results for a magnetic field intensity of 5960 A/m, a surface tension coefficient (σ) of 0.0135 N/m, and a magnetic susceptibility (χ) of 0.89, which were kept constant.

To evaluate how our conservative level set method compares with the S-CLSVOF method used by Ghaffari et al. [36], a comparison was made between the results of both methods and the theoretical predictions from Eq. (18). This comparison is depicted in Fig. 10.

5.3. The effect of surface tension coefficient

This part of the study examines the impact of the surface tension parameter on the shape transformation of ferrofluid when exposed to a homogeneous magnetic field with an intensity of 5960 A/m. Unlike the case discussed in Section 5.1, where the droplet had a magnetic susceptibility of 0.89 and a radius of 1.291 mm, the impact of surface tension forces is more prominent here compared to the magnetic forces (see Supplementary Fig. S6).

The height-to-width ratio of the ferrofluid droplet depends on the Bond number. When the surface tension coefficient increases, the Bond number decreases, which causes the droplet to become more circular rather than elliptical. This results in aspect ratio decreasing and approaching 1, as illustrated in Fig. 11. Fig. 12 compares the aspect ratios from our simulation with those obtained using the S-CLSVOF method.

As discussed earlier, we compared the results of conservative level set method and the S-CLSVOF approach with the theoretical values from Eq. (18). The comparison diagrams are shown in Fig. 13.

5.4. The influence of magnetic susceptibility

By assuming a constant Bond number, magnetic susceptibility becomes a crucial parameter influencing the shape transformation of the ferrofluid. Additionally, magnetic susceptibility is a dimensionless quantity that indicates the extent to which a substance becomes magnetized when exposed to an external magnetic field. To examine how magnetic susceptibility affects the droplet's shape, we simulated cases with magnetic susceptibilities ranging from 0.25 to 5, using an initial droplet radius of 1.291 mm. These results are

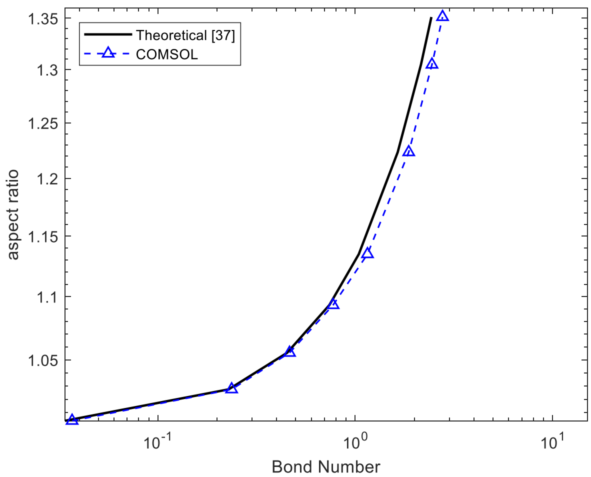

Fig. 8. A comparison of the simulation and theoretical predictions concerning the shape ratio in relation to different Bond numbers.

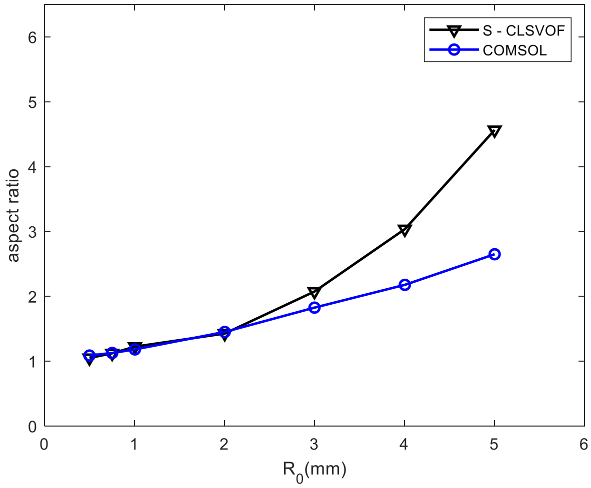

Fig. 9. A comparison of the aspect ratio of COMSOL simulation with the S-CLSVOF method subjected to homogeneous magnetic field with various initial radii.

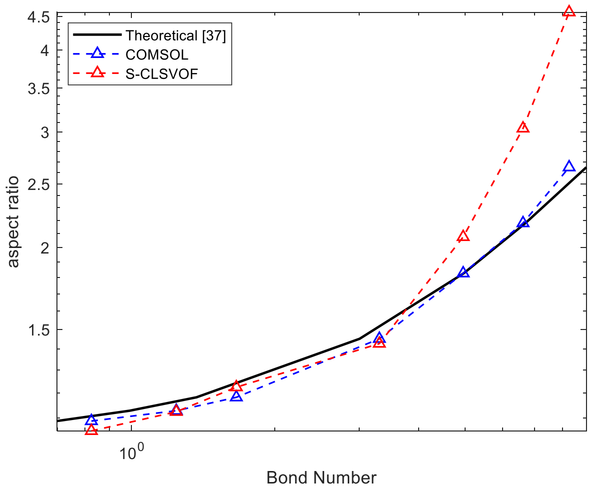

Fig. 10. A graph to compare the conservative level set method and S-CLSVOF approach with theory for different initial radii.

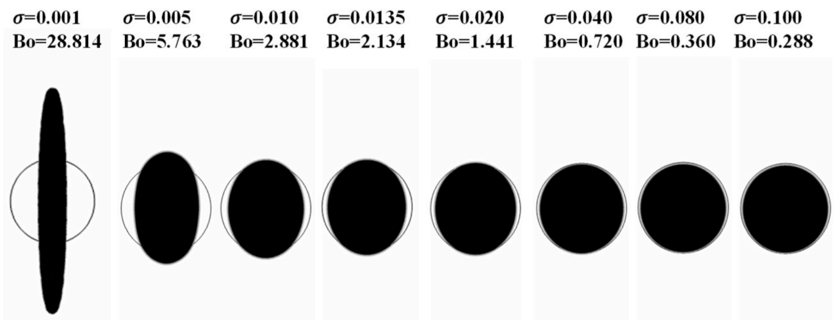

Fig. 11. Shape transformation of ferrofluid subjected to homogeneous magnetic actuation and the associated surface tension coefficient.

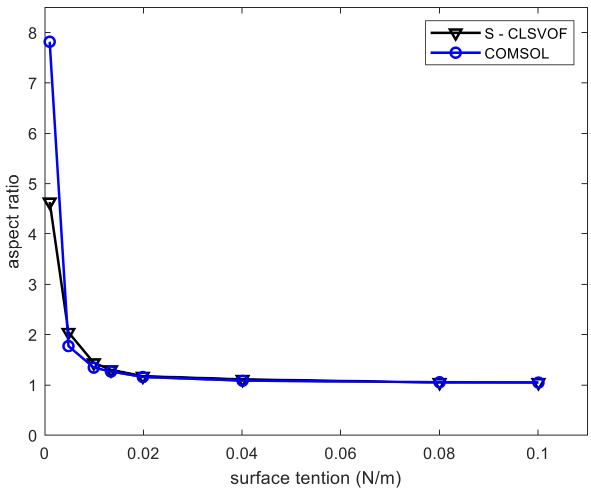

Fig. 12. A comparison between the aspect ratio of COMSOL simulation with the S-CLSVOF method under the constant homogeneous magnetic field.

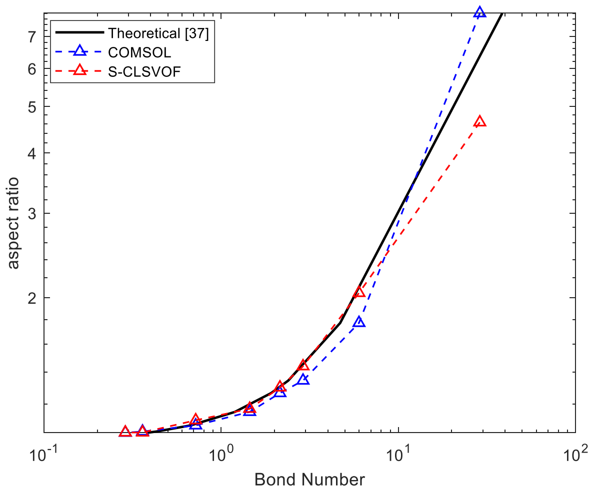

Fig. 13. The impact of surface tension parameter on the conservative level set, S-CLSVOF and theoretical approach.

shown in Fig. 14. We also compared these simulations with the S-CLSVOF method by varying the initial droplet radius to 0.75 mm, 1.2191 mm, 2 mm, and 3 mm, as illustrated in Fig. 15. Fig. 14 shows that as magnetic susceptibility increases, the shape transformation of ferrofluid becomes more pronounced. For a magnetic susceptibility of $\chi = 3$, the droplet significantly deforms into an elliptical shape with conical ends. Fig. 15 reveals that for magnetic susceptibilities below 1, the droplet deformation is minimal. However, at

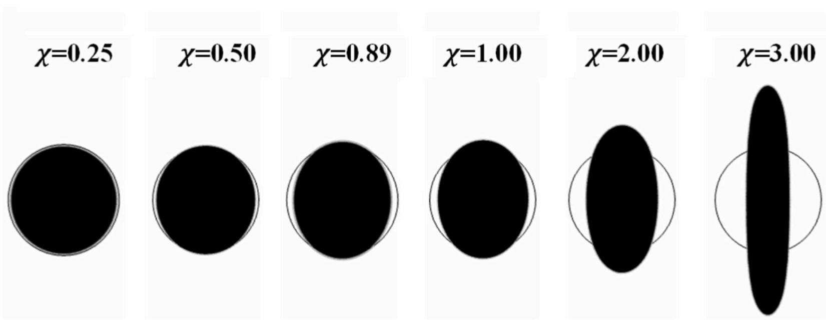

Fig. 14. Illustration of the shape transformation of ferrofluid having an initial radius of 1.291 mm under uniform magnetic field and different magnetic susceptibility values.

higher susceptibilities, increasing the initial radius leads to a notable increase in the aspect ratio.

We also used theoretical calculations to evaluate the outcomes obtained from conservative level set numerical method for two different magnetic susceptibilities, as shown in Fig. 16.

5.5. Investigating the influence of the external magnetic actuation on the coalescence of two ferrofluid droplets under gravity

When two ferrofluid droplets are placed in a weakly magnetic liquid and subjected to an external magnet, they act like magnetic dipoles and attract each other. This attraction grows stronger as the droplets move closer together, eventually causing them to merge. The attraction occurs because the ferrofluid converts the uniform magnetic field around it into a non-uniform field, creating a magnetic field gradient. Additionally, gravity pulls the droplets downward. The current simulation model differs from the previous models. As shown in Fig. 17A, this model includes two droplets with an initial radius of 1 mm, a center-to-center distance of 4 mm, and properties such as density of 1260 kg/m^3 and viscosity of 0.1 Pa s placed in a non-magnetic fluid with a lower density of 966 kg/m^3 and the same viscosity as the previous system. The magnetic field, directed along the direction of gravity, has an intensity of $H_0 = 10{,}000$ A/m, as depicted in Fig. 17B.

Wörner [46] examined numerical techniques used to model and track the interface during droplet coalescence and claimed that the standard level set method could not accurately represent more than one interface inside a single computational grid cell. However, by modifying the level set method, the coalescence of two ferrofluid droplets were simulated successfully.

As shown in Fig. 18, The two ferrofluid droplets were initially stretched along the magnetic field's direction. As the magnetic attraction among the droplets intensifies, they merge at 0.24 s and then fall under the influence of gravity. Fig. 18 illustrates that the attraction forces between the two droplets are equal in magnitude ($|F12| = |F21|$). Since the droplets have the same shape and mass, the gravitational force acting on each is also the same. However, because the F21 is parallel to gravity, droplet 1 (i.e., the upper one) accelerates more and falls faster than droplet 2 (i.e., the lower one). To better understand the impact of the magnetic actuation, we repeated the simulation subjected to gravity in the absence of magnetic field. As depicted in Fig. 19, in the absence of magnetic actuation, the droplets fall solely due to gravity, and no deformation, collision, or merging is observed.

5.6. 3D model of ferrofluid droplet deformation subjected to different intensities of homogeneous magnetic actuation

The conservative level set approach can be extended to 3D environments [44]. Therefore, we investigate the shape-shifting of a ferrofluid droplet in a 3D model exposed to different homogeneous magnetic field intensities.

To simulate the three-dimensional deformation of a ferrofluid droplet, we extend the conservative level set technique and adapt the 2D magnetic stress tensor equation to three dimensions. The updated version of Eq. (11) for the 3D case is according to Eq. (19):

$$\tau_m = \mu\left(\mathbf{H}_i\mathbf{H}_j - \frac{\delta_{ij}}{2}H^2\right), \delta_{ij} = \begin{cases} 1 & i = j \\ 0 & i \neq j \end{cases} \tag{19}$$

This definition for the magnetic stress tensor was provided by Afkhami et al. [37]. It could be rewritten as Eq. (20):

$$\tau_m = \mu \begin{bmatrix} \mathbf{H}_x^2 - \frac{1}{2}H^2 & \mathbf{H}_x\mathbf{H}_y & \mathbf{H}_x\mathbf{H}_z \\ \mathbf{H}_x\mathbf{H}_y & \mathbf{H}_y^2 - \frac{1}{2}H^2 & \mathbf{H}_y\mathbf{H}_z \\ \mathbf{H}_x\mathbf{H}_z & \mathbf{H}_y\mathbf{H}_z & \mathbf{H}_z^2 - \frac{1}{2}H^2 \end{bmatrix} \tag{20}$$

Using Eq. (20) and Eq. (10), we can calculate the magnetic forces acting on the three-dimensional model of the ferrofluid droplet. For our simulation, we consider a cube with a side length of 1 cm and place a ferrofluid droplet inside it. We apply a constant magnetic field along the y axis with different intensities: 2500 A/m, 5960 A/m, and 10000 A/m. The results of these simulations are shown in Fig. 20, which includes isometric, front, top, and right views of the droplet in its equilibrium state for each magnetic field intensity.

6. Conclusion

We successfully simulated a ferrofluid droplet subjected to homogeneous magnetic field using a conservative level set numerical approach in COMSOL. Our study demonstrated that enhancements to the level set method, specifically the conservative level set approach, enable accurate simulation of droplet coalescence and extend its applicability to scenarios like emulsion breakage. Furthermore, the conservative level set technique outperformed both the VOF method and the S-CLSVOF method, a simple coupling of level set and VOF techniques.

Compared to other numerical methods, our simulation shows strong agreement with experimental data, even under high magnetic field intensities. The biomedical applications of ferrofluids and the demands of high magnetic field environments require precise

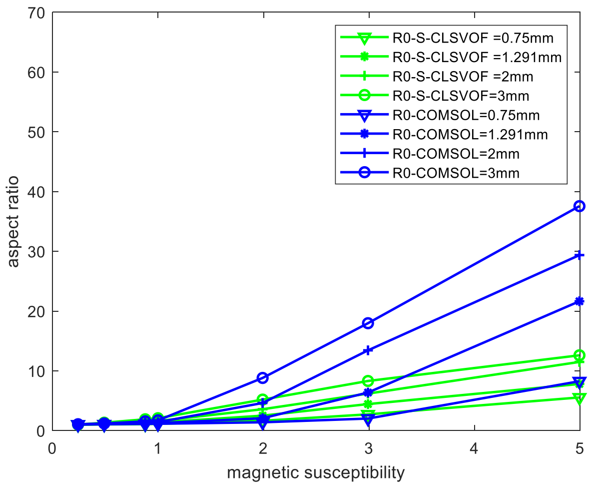

Fig. 15. A comparison between the aspect ratio of COMSOL simulation with the S-CLSVOF method under the constant uniform magnetic field and different values of.

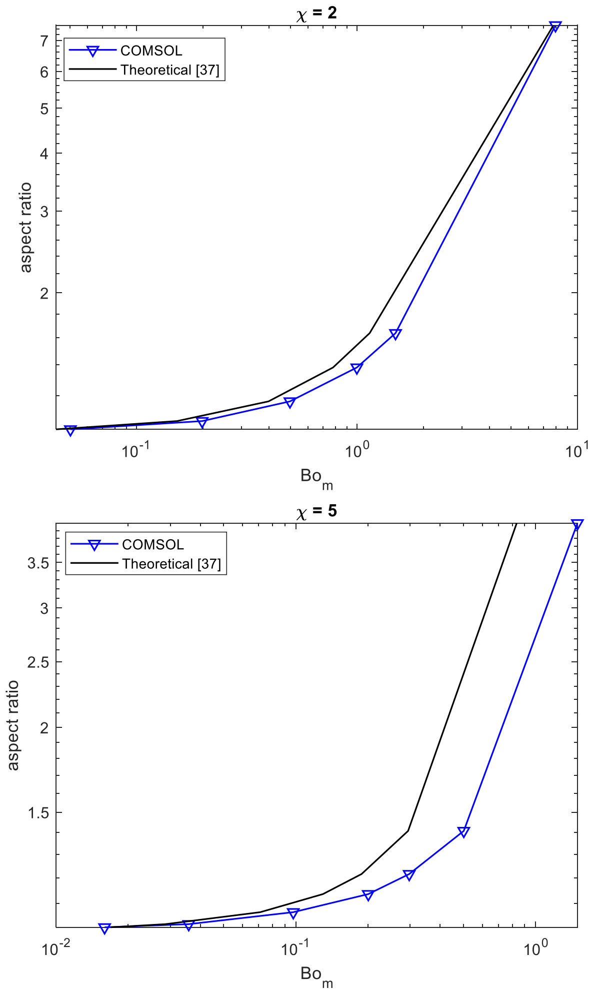

Fig. 16. Comparison between the results of COMSOL and the theory for two different magnetic susceptibilities, $\chi = 2$ and $\chi = 5$.

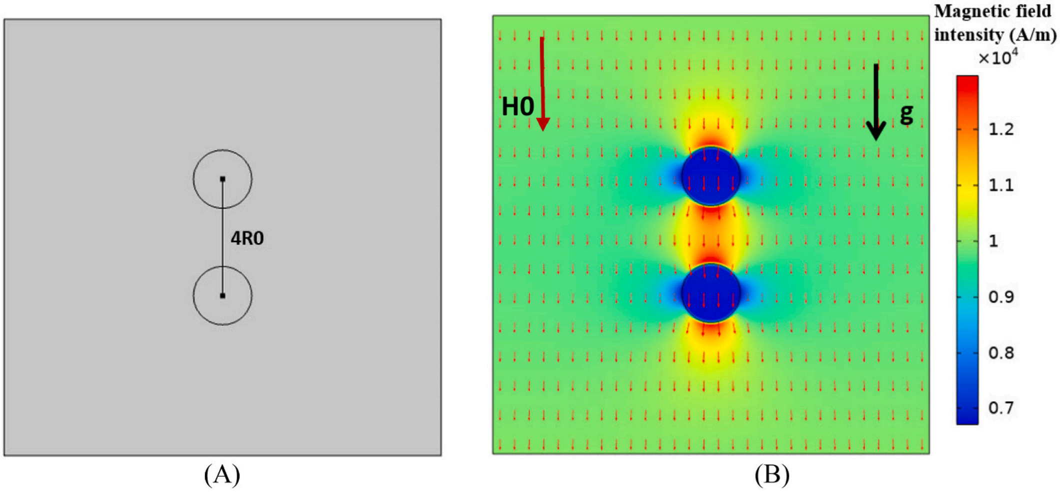

Fig. 17. Merging simulation of two ferrofluid droplets subjected to homogeneous magnetic field. (A) Geometry model. (B) Magnetic field and gravitational acceleration direction.

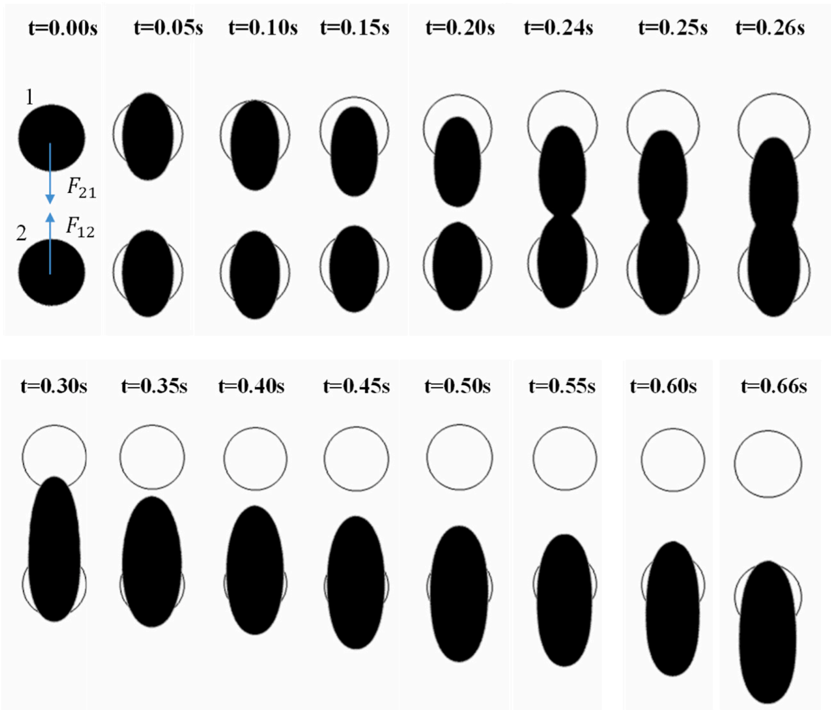

Fig. 18. Merging of two ferrofluid droplets under an external magnetic field and gravity.

dynamic modeling. This paper addresses the crucial task of establishing a framework for more accurate ferrofluid modeling under the influence of magnetic fields, enabling the extraction of governing dynamics for designing model-based controllers [47,48], Thus, ensuring the stability and desired response of such model-based controllers is crucial, especially in high-risk environments such as human tissue.

Future work will focus on examining how additional parameters act on the deformation of 3D ferrofluid droplets using COMSOL, with the goal of achieving greater simulation accuracy than has been achieved so far. Our two-dimensional and three-dimensional models will help address the control of ferrofluid droplets along specific trajectories using magnetic actuation, ultimately advancing the development of wireless ferrofluidic microrobots for biomedical applications.

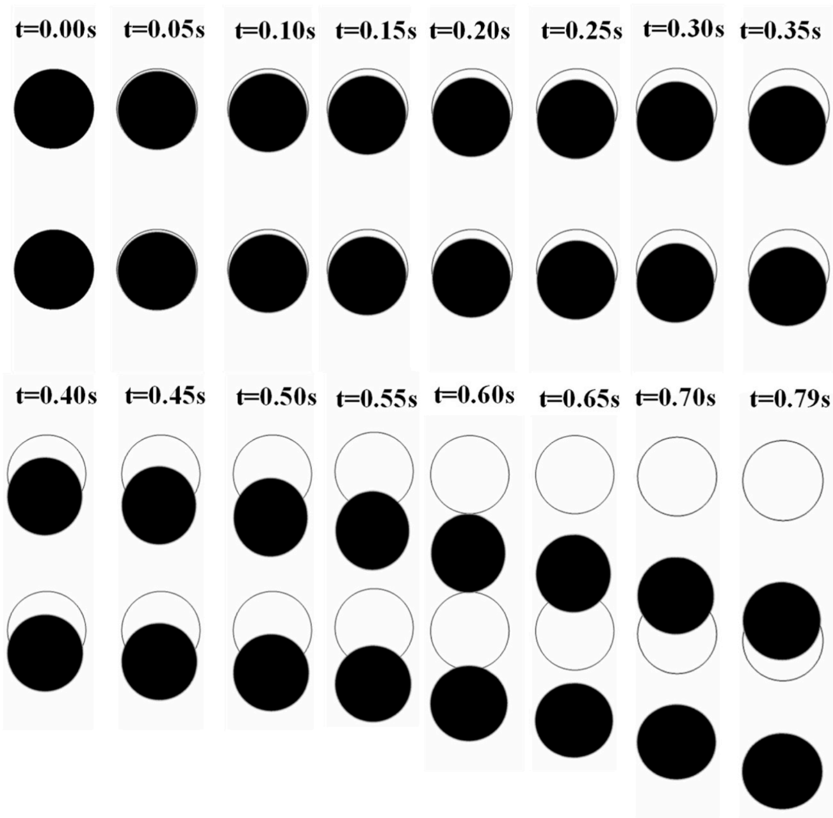

Fig. 19. Fall of two ferrofluid droplets under gravity.

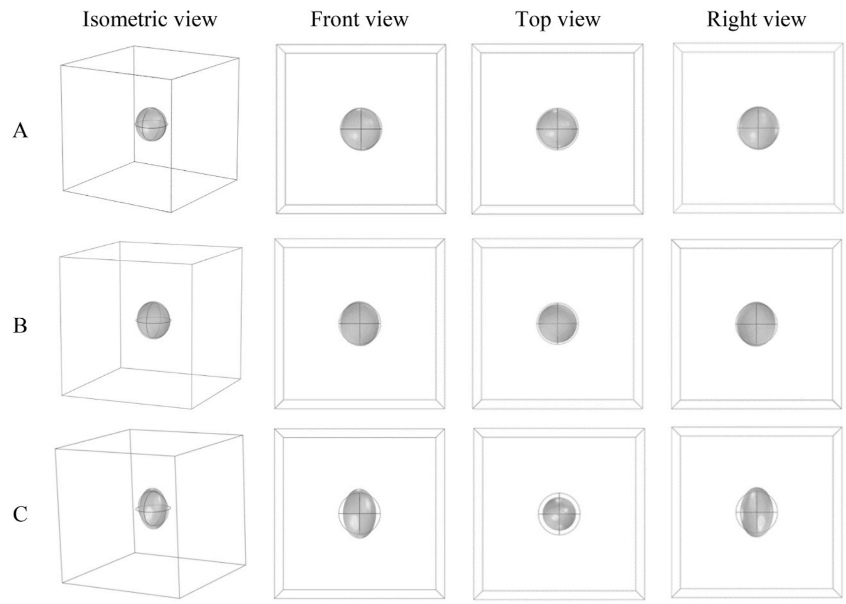

Fig. 20. 3D model of ferrofluid droplet subjected to different values of homogeneous magnetic fields A) H0 = 2500 A/m. B) H0 = 5960 A/m. C) H0 = 10000 A/m.

CRediT authorship contribution statement

Mobina Taghaddosi: Writing – original draft, Validation, Software, Methodology, Formal analysis. **Mobin Salehi:** Writing – review & editing, Validation, Software. **Borhan Beigzadeh:** Writing – review & editing, Project administration, Methodology, Conceptualization.

Data availability

The data supporting this study's findings are available from the corresponding author upon reasonable request.

Declaration of competing interest

The authors declare that they have no known competing financial interests or personal relationships that could have appeared to influence the work reported in this paper.

Appendix A. Supplementary data

Supplementary data to this article can be found online at https://doi.org/10.1016/j.heliyon.2024.e40111.

References

[1] R.E. Rosensweig, Directions in Ferrohydrodynamics, J. Appl. Phys. 57 (1985) 4259–4264, https://doi.org/10.1063/1.334579.
[2] G. Kandasamy, S. Soni, K. Sushmita, N.S. Veerapu, S. Bose, D. Maity, One-step synthesis of hydrophilic functionalized and cytocompatible superparamagnetic iron oxide nanoparticles (SPIONs) based aqueous ferrofluids for biomedical applications, J. Mol. Liq. 274 (2019) 653–663, https://doi.org/10.1016/j.molliq.2018.10.161.
[3] F. Jiao, Q. Li, Y. Jiao, Y. He, Heat transfer of ferrofluids with magnetoviscous effects, J. Mol. Liq. 328 (2021) 115404, https://doi.org/10.1016/j.molliq.2021.115404.
[4] M. Khani, M. Haghshenasfard, N. Etesami, M.R. Talaei, CO2 absorption using ferrofluids in a venturi scrubber with uniform magnetic field of a solenoid, J. Mol. Liq. 334 (2021) 116078, https://doi.org/10.1016/j.molliq.2021.116078.
[5] S. Shyam, U. Banerjee, P.K. Mondal, S.K. Mitra, Impact dynamics of ferrofluid droplet on a PDMS substrate under the influence of magnetic field, Colloids Surf. A Physicochem. Eng. Asp. 661 (2023) 130911, https://doi.org/10.1016/j.colsurfa.2022.130911.
[6] S. Shyam, A. Yadav, Y. Gawade, et al., Dynamics of a single isolated ferrofluid plug inside a micro-capillary in the presence of externally applied magnetic field, Exp Fluids 61 (2020) 210, https://doi.org/10.1007/s00348-020-03043-0.
[7] M. Kole, S. Khandekar, Engineering applications of ferrofluids: a review, J. Magn. Magn Mater. 537 (February) (2021) 168222, https://doi.org/10.1016/j.jmmm.2021.168222.
[8] V.B. Varma, et al., Control of ferrofluid droplets in microchannels by uniform magnetic fields, IEEE Magn. Lett. 7 (i) (2016) 1–5, https://doi.org/10.1109/LMAG.2016.2594165.
[9] Z. Wang, V.B. Varma, H.M. Xia, Z.P. Wang, R.V. Ramanujan, Spreading of a ferrofluid core in three-stream micromixer channels, Phys. Fluids 27 (5) (2015) 1–11, https://doi.org/10.1063/1.4919927.
[10] S. Wang, H. Liu, W. Xu, Hydrodynamic modelling and CFD simulation of ferrofluids flow in magnetic targeting drug delivery, Int. J. Comut. Fluid Dyn. 22 (10) (2008) 659–667, https://doi.org/10.1080/10618560802452009.
[11] M. Ilami, R.J. Ahmed, A. Petras, B. Beigzadeh, H. Marvi, Magnetic needle steering in soft phantom tissue, Sci. Rep. 10 (1) (2020) 1–11, https://doi.org/10.1038/s41598-020-59275-x.
[12] L. Hajba, A. Guttman, Circulating tumor-cell detection and capture using microfluidic devices, TrAC - Trends Anal. Chem. 59 (2014) 9–16, https://doi.org/10.1016/j.trac.2014.02.017.
[13] J. Burgner-Kahrs, D.C. Rucker, H. Choset, Continuum robots for medical applications: a survey, IEEE Trans. Robot. 31 (6) (2015) 1261–1280, https://doi.org/10.1109/TRO.2015.2489500.
[14] H.D. Liu, W. Xu, S.G. Wang, Z.J. Ke, Hydrodynamic modeling of ferrofluid flow in magnetic targeting drug delivery, Appl. Math. Mech. 29 (10) (2008) 1341–1349, https://doi.org/10.1007/s10483-008-1009-y.
[15] B. Beigzadeh, M. Halabian, Effect of static magnetic field on the hemodynamic properties of blood flow containing magnetic substances, J. Comput. Appl. Mech. 47 (2) (2016) 181–194, https://doi.org/10.22059/jcamech.2017.202240.101.
[16] B. Beigzadeh, A. Rasaeifard, Homotopy-based solution of Navier-Stokes equations for two-phase flow during magnetic drug targeting, J. Mol. Liq. 238 (2017) 11–18, https://doi.org/10.1016/j.molliq.2017.04.106.
[17] H. Aryan, B. Beigzadeh, M. Siavashi, Euler-Lagrange numerical simulation of improved magnetic drug delivery in a three-dimensional CT-based carotid artery bifurcation, Comput. Methods Programs Biomed. 219 (2022) 106778, https://doi.org/10.1016/j.cmpb.2022.106778.
[18] R. Ahmed, M. Ilami, J. Bant, B. Beigzadeh, H. Marvi, A shapeshifting ferrofluidic robot, Soft Robot. 00 (00) (2020) 1–12, https://doi.org/10.1089/soro.2019.0184.
[19] S. Shyam, P.K. Mondal, B. Mehta, Magnetofluidic mixing of a ferrofluid droplet under the influence of a time-dependent external field, J. Fluid Mech. 917 (2021) A15, https://doi.org/10.1017/jfm.2021.245.
[20] C. Flament, S. Lacis, J.C. Bacri, A. Cebers, S. Neveu, R. Perzynski, Measurements of ferrofluid surface tension in confined geometry, Phys. Rev. E - Stat. Physics, Plasmas, Fluids, Relat. Interdiscip. Top. 53 (5) (1996) 4801–4806, https://doi.org/10.1103/PhysRevE.53.4801.
[21] W.K. Lee, R. Scardovelli, A.D. Trubatch, P. Yecko, Numerical, experimental, and theoretical investigation of bubble aggregation and deformation in magnetic fluids, Phys. Rev. E - Stat. Nonlinear Soft Matter Phys. 82 (1) (2010), https://doi.org/10.1103/PhysRevE.82.016302.
[22] O. Lavrova, G. Matthies, T. Mitkova, V. Polevikov, L. Tobiska, Numerical treatment of free surface problems in ferrohydrodynamics, J. Phys. Condens. Matter 18 (38) (2006), https://doi.org/10.1088/0953-8984/18/38/S09.
[23] S. Osher, J.A. Sethian, Fronts propagating with curvature-dependent speed: algorithms based on Hamilton-Jacobi formulations, J. Comput. Phys. 79 (1) (1988) 12–49, https://doi.org/10.1016/0021-9991(88)90002-2.
[24] J. Liu, Y.F. Yap, N.T. Nguyen, Numerical study of the formation process of ferrofluid droplets, Phys. Fluids 23 (7) (2011), https://doi.org/10.1063/1.3614569.
[25] L.H.P. Cunha, I.R. Siqueira, T.F. Oliveira, H.D. Ceniceros, Field-induced control of ferrofluid emulsion rheology and droplet break-up in shear flows, Phys. Fluids 30 (12) (2018), https://doi.org/10.1063/1.5055943.

[26] S. Shyam, B. Dhapola, P.K. Mondal, Magnetofluidic-based controlled droplet breakup: effect of non-uniform force field, J. Fluid Mech. 944 (2022) A51, https://doi.org/10.1017/jfm.2022.504.
[27] M.R. Hassan, J. Zhang, C. Wang, Deformation of a ferrofluid droplet in simple shear flows under uniform magnetic fields, Phys. Fluids 30 (9) (2018), https://doi.org/10.1063/1.5047223.
[28] V.G.E. Abicalil, R.F. Abdo, L.H.P. Da Cunha, T.F. De Oliveira, On the magnetization of dilute ferrofluid emulsions in shear flows, Phys. Fluids 33 (5) (2021), https://doi.org/10.1063/5.0050643.
[29] S. Afkhami, Y. Renardy, M. Renardy, J.S. Riffle, T.G.S. Pierre, Numerical modeling of ferrofluid droplets in magnetic fields, AIP Conf. Proc. 1027 (1) (2008) 884–886, https://doi.org/10.1063/1.2964882.
[30] Y. Hu, D. Li, X. Niu, Phase-field-based lattice Boltzmann model for multiphase ferrofluid flows, Phys. Rev. E 98 (3) (2018), https://doi.org/10.1103/PhysRevE.98.033301.
[31] Shi-Ting Zhang, Xiao-Dong Niu, Qian-Ping Li, Adnan Khan, Yang Hu, De-Cai Li, A numerical investigation on the deformation of ferrofluid droplets, Phys. Fluids 35 (1) (2023) 012102, https://doi.org/10.1063/5.0131884.
[32] Q. He, W. Huang, J. Xu, Y. Hu, D. Li, A hybrid immersed interface and phase-field-based lattice Boltzmann method for multiphase ferrofluid flow, Computers & Fluids 255 (2023) 105821, https://doi.org/10.1016/j.compfluid.2023.105821.
[33] D. Shi, Q. Bi, R. Zhou, Numerical simulation of a falling ferrofluid droplet in a uniform magnetic field by the VOSET method, Numer. Heat Transf. Part A Appl. 66 (2) (2014) 144–164, https://doi.org/10.1080/10407782.2013.869459.
[34] D.L. Sun, W.Q. Tao, A coupled volume-of-fluid and level set (VOSET) method for computing incompressible two-phase flows, Int. J. Heat Mass Transf. 53 (4) (2010) 645–655, https://doi.org/10.1016/j.ijheatmasstransfer.2009.10.030.
[35] A. Albadawi, D.B. Donoghue, A.J. Robinson, D.B. Murray, Y.M.C. Delauré, Influence of surface tension implementation in Volume of Fluid and coupled Volume of Fluid with Level Set methods for bubble growth and detachment, Int. J. Multiph. Flow 53 (2013) 11–28, https://doi.org/10.1016/j.ijmultiphaseflow.2013.01.005.
[36] A. Ghaffari, S.H. Hashemabadi, M. Bazmi, CFD simulation of equilibrium shape and coalescence of ferrofluid droplets subjected to uniform magnetic field, Colloids Surfaces A Physicochem. Eng. Asp. 481 (2015) 186–198, https://doi.org/10.1016/j.colsurfa.2015.04.038.
[37] S. Afkhami, et al., Deformation of a hydrophobic ferrofluid droplet suspended in a viscous medium under uniform magnetic fields, J. Fluid Mech. 663 (2010) 358–384, https://doi.org/10.1017/S0022112010003551.
[38] Z. Chen, C. Shu, D. Tan, X.D. Niu, Q.Z. Li, Simplified multiphase lattice Boltzmann method for simulating multiphase flows with large density ratios and complex interfaces, Phys. Rev. E 98 (6) (2018) 1–18, https://doi.org/10.1103/PhysRevE.98.063314.
[39] A. Khan, X.D. Niu, Y. Li, M.F. Wen, D.C. Li, H. Yamaguchi, Motion, deformation, and coalescence of ferrofluid droplets subjected to a uniform magnetic field, Int. J. Numer. Methods Fluids 92 (11) (2020) 1584–1603, https://doi.org/10.1002/fld.4840.
[40] M. Majidi, M.A. Bijarchi, A.G. Arani, M.H. Rahimian, M.B. Shafii, Magnetic field-induced control of a compound ferrofluid droplet deformation and breakup in shear flow using a hybrid lattice Boltzmann-finite difference method, Int. J. Multiph. Flow 146 (January) (2022), https://doi.org/10.1016/j.ijmultiphaseflow.2021.103846.
[41] S.E. Borglin, G.J. Moridis, C.M. Oldenburg, Experimental studies of the flow of ferrofluid in porous media, Transp. Porous Media 41 (1) (2000) 61–80, https://doi.org/10.1023/A:1006676931721.
[42] M. Sussman, A level set approach for computing solutions to incompressible two-phase flow, J. Comput. Phys. 114 (1) (1994) 146–159, https://doi.org/10.1006/jcph.1994.1155.
[43] A.-K. Tornberg, B. Engquist, M. Espedal, A. Quarteroni, Computing and Visualization in Science A finite element based level-set method for multiphase flow applications, Comput Vis. Sci 3 (2000) 93–101.
[44] E. Olsson, G. Kreiss, A conservative level set method for two phase flow, J. Comput. Phys. 210 (1) (2005) 225–246, https://doi.org/10.1016/j.jcp.2005.04.007.
[45] P.A. Voltairas, D.I. Fotiadis, L.K. Michalis, Hydrodynamics of magnetic drug targeting, J. Biomech. 35 (6) (2002) 813–821, https://doi.org/10.1016/S0021-9290(02)00034-9.
[46] M. Wörner, Numerical modeling of multiphase flows in microfluidics and micro process engineering: a review of methods and applications, Microfluid. Nanofluidics 12 (6) (2012) 841–886, https://doi.org/10.1007/s10404-012-0940-8.
[47] A. Rezvanian, B. Beigzadeh, A.H. Davaei Markazi, M. Halabian, Feedback control of temperature in specific geometry of porous media: application to hyperthermia, J. Therm. Anal. Calorim. 141 (5) (2020) 1559–1568, https://doi.org/10.1007/s10973-020-09597-9.
[48] M. Sun, B. Hao, S. Yang, X. Wang, C. Majidi, L. Zhang, Exploiting ferrofluidic wetting for miniature soft machines, Nat. Commun. 2022 131 13 (1) (2022) 1–14, https://doi.org/10.1038/s41467-022-35646-y.